

Are your MRI contrast agents cost-effective?

Learn more about generic Gadolinium-Based Contrast Agents.



**AJNR**

**Quantification of Cerebrovascular Reactivity by Blood Oxygen Level –Dependent MR Imaging and Correlation with Conventional Angiography in Patients with Moyamoya Disease**

This information is current as of April 17, 2024.

C. Heyn, J. Poublanc, A. Crawley, D. Mandell, J.S. Han, M. Tymianski, K. terBrugge, J.A. Fisher and D.J. Mikulis

*AJNR Am J Neuroradiol* 2010, 31 (5) 862-867

doi: <https://doi.org/10.3174/ajnr.A1922>

<http://www.ajnr.org/content/31/5/862>

**ORIGINAL  
RESEARCH**

C. Heyn  
J. Poubanc  
A. Crawley  
D. Mandell  
J.S. Han  
M. Tymianski  
K. terBrugge  
J.A. Fisher  
D.J. Mikulis

# Quantification of Cerebrovascular Reactivity by Blood Oxygen Level–Dependent MR Imaging and Correlation with Conventional Angiography in Patients with Moyamoya Disease

**BACKGROUND AND PURPOSE:** BOLD MR imaging combined with a technique for precision control of end-tidal  $p\text{CO}_2$  was used to produce quantitative maps of CVR in patients with Moyamoya disease. The technique was validated against measures of disease severity by using conventional angiography; it then was used to study the relationship between CVR, vascular steal, and disease severity.

**MATERIALS AND METHODS:** A retrospective analysis comparing conventional angiography with BOLD MR imaging was performed on 11 patients with Moyamoya disease. Iso-oxic cycling of end-tidal  $p\text{CO}_2$  between 2 target values was performed during BOLD MR imaging. CVR was calculated as the BOLD signal difference per  $\Delta p\text{CO}_2$ . CVR was correlated with the presence of Moyamoya or pial collaterals and the degree of Moyamoya disease as graded by using a modified Suzuki score.

**RESULTS:** A good correlation between mean CVR and Suzuki score was found for the MCA and ACA territories (Pearson correlation coefficient,  $-0.7560$  and  $-0.6140$ , respectively;  $P < .0001$ ). A similar correlation was found between mean CVR and the presence of pial and Moyamoya collateral vessels for combined MCA and ACA territories (Pearson correlation coefficient,  $-0.7466$ ;  $P < .0001$ ). On a voxel-for-voxel basis, there was a greater extent of steal within vascular territories with increasing disease severity (higher modified Suzuki score). Mean CVR was found to scale nonlinearly with the extent of vascular steal.

**CONCLUSIONS:** Quantitative measures of CVR show direct correlation with impaired vascular supply as measured by the modified Suzuki score and enable direct investigation of the physiology of autoregulatory reserve, including steal phenomenon, within a given vascular territory.

**ABBREVIATIONS:** ACA = anterior cerebral artery; AFNI = analysis of functional neuroimages; AIF = arterial input function; ANOVA = analysis of variance; BOLD = blood oxygen level–dependent; CBF = cerebral blood flow; CVR = cerebrovascular reactivity;  $\text{CO}_2$  = carbon dioxide;  $\Delta\text{SpCO}_2$  = difference per change in end-tidal carbon dioxide;  $f$  = fraction; ICA = internal carotid artery; MCA = middle cerebral artery; neg = negative; PCA = posterior cerebral artery;  $p\text{CO}_2$  = partial pressure of carbon dioxide; PET = positron-emission tomography;  $p\text{O}_2$  = partial pressure of oxygen; pos = positive; SE = standard error; SPECT = single-photon emission CT; TIA = transient ischemic attack

**M**oyamoya disease is a vasculopathy affecting the proximal circle of Willis vessels characterized by progressive narrowing and formation of secondary collaterals. Blood flow distal to these stenotic vessels is thought to be maintained by a drop in vascular resistance mediated by small artery and arteriolar vasodilation. As the disease progresses, however, the ability of this autoregulatory system or CVR to preserve adequate perfusion is lost when compensatory arteriolar dilation reaches a maximum. Further increases in vascular resistance at the stenosis ultimately lead to tissue oligemia and possible

ischemia. Measurements of CVR can provide valuable information for planning surgical revascularization, assessing the success of such a procedure postoperatively, and predicting the recurrence of focal neurologic symptoms.<sup>1</sup>

$\text{CO}_2$  is a potent vasodilator of the cerebrovasculature and can be used to test the responsiveness of the autoregulatory system in patients with Moyamoya disease. Measurements of regional CBF in response to changes in end-tidal  $p\text{CO}_2$  have been accomplished with a number of imaging modalities, including PET,<sup>2</sup> SPECT,<sup>3</sup> CT perfusion,<sup>4</sup> and MR imaging. BOLD MR imaging measurement of CVR, in particular, has recently been shown to be highly correlated with CBF in patients with steno-occlusive disease caused by atherosclerosis or Moyamoya disease.<sup>5</sup>

Blood flow manipulation is typically achieved by acetazolamide stress, breath-hold techniques, or steady-state  $\text{CO}_2$  administration via a face mask. These methods produce inconsistent changes in blood flow. Recently, we have implemented a method for precision control of end-tidal  $p\text{CO}_2$  and  $p\text{O}_2$ ,<sup>6</sup> permitting accurate correlation of changes in  $p\text{CO}_2$  with the BOLD MR imaging signal-intensity response.

In the present work, we used BOLD MR imaging in combination with precise iso-oxic changes in end-tidal  $\text{CO}_2$  to

Received June 4, 2009; accepted after revision September 16.

From the Departments of Medical Imaging (C.H., J.P., A.C., D.M., K.t.B., D.J.M.) and Surgery (M.T.), Division of Neurosurgery, Toronto Western Hospital of the University Health Network, Toronto, Ontario, Canada; Department of Anesthesia (J.S.H., J.A.F.), University Health Network, Toronto, Ontario, Canada; and Department of Physiology (J.S.H.), University of Toronto, Toronto, Ontario, Canada.

J.A.F. and D.J.M. contributed to the development of the RespirAct, a device used in this study. These authors stand to benefit financially if this device is successfully commercialized by Thornhill Research, a University of Toronto/University Health Network–related company.

Please address correspondence to David J. Mikulis, MD, Department of Medical Imaging, Toronto Western Hospital, Rm 3MC-431, 399 Bathurst St, Toronto, ON, Canada. L6J 7P9; e-mail: mikulis@uhnres.utoronto.ca

DOI 10.3174/ajnr.A1922

**Clinical and angiographic characteristics of 11 patients<sup>a</sup>**

Case No.	Age (yr)	Sex	Clinical Presentation	Suzuki		Collaterals ACA		Collaterals MCA		Collaterals PCA	
				Left	Right	Left	Right	Left	Right	Left	Right
1	48	F	Headache	0	III	0	0	0	2	0	0
2	36	M	Headache	0	III	0	0	0	2	0	0
3	45	M	TIA (left weakness)	II	IV	2	2	0	2	0	0
4	39	F	TIA (right weakness)	II	0	0	0	2	0	0	0
5	33	F	Headache	II	II	2	1	1	1	0	0
6	35	F	TIA (left weakness)	IV	IV	2	2	1	1	1	1
7	44	M	Right facial, arm numbness, slurred speech	IV	0	0	0	2	0	0	0
8	41	M	TIA (right weakness)	IV	III	0	1	2	2	0	0
9	10	F	Asymptomatic	IV	0	1	0	2	0	0	0
10	11	F	TIA (right hand weakness)	IV	IV	2	2	2	2	0	0
11	33	F	Asymptomatic	III	II	2	2	2	2	0	1

<sup>a</sup> 0 indicates no collaterals (M-P-); 1, Moyamoya collaterals only (M+P-); 2, pial and Moyamoya collaterals (M+P+).

produce quantitative maps of CVR in patients with Moyamoya disease. To validate this technique, we correlated measurements of CVR with a modified Suzuki score, which is a measure of disease severity determined by using conventional angiography. The measures of CVR were also correlated with the extent of steal within a vascular territory, providing insight into the physiology of autoregulatory reserve.

**Materials and Methods**

**Patient Selection and Angiographic Scoring**

A retrospective analysis was performed on patients with Moyamoya disease undergoing cerebrovascular reactivity measurements before surgical revascularization at our institution. Ethics approval was obtained through our research institute’s ethics committee and written consent was given by all participants. Patients without structural brain disease such as ischemic or hemorrhagic stroke and those with a prior conventional angiogram with 6-vessel injection obtained within 6 months before the CVR study were included in the study. A total of 11 patients who underwent a CVR study between October 2005 and June 2007 were evaluated.

The degree of Moyamoya disease as visualized on conventional angiography was scored by a neuroradiologist (D.J.M.) using a modified Suzuki score<sup>7</sup>: stage 0, no evidence of vessel disease; stage I, mild-to-moderate stenosis around the carotid bifurcation with absent or slightly developed ICA Moyamoya disease (almost all of both ACA and MCA branches are opacified in antegrade fashion); stage II, severe stenosis around the carotid bifurcation or occlusion of either the proximal ACA or MCA with well-developed ICA Moyamoya disease (either the ACA or MCA branches or both are clearly defective, but at least several of the ACA or MCA branches remain opacified in antegrade fashion); stage III, occlusion of both the proximal ACA and MCA with well-developed ICA Moyamoya disease (only a few of either the ACA or MCA branches or both are faintly opacified in antegrade fashion through the meshwork of ICA Moyamoya disease); and stage IV, complete occlusion of both the proximal ACA and MCA with an absent or a small amount of ICA Moyamoya disease (without opacification of either the ACA or MCA branches in antegrade fashion).

Each vascular territory was also assessed for the presence of Moyamoya or leptomeningeal collaterals. For the purpose of scoring these collaterals, a simple binary system was used (M-P- to indicate the absence of Moyamoya or pial collaterals, M+P- to indicate the presence of Moyamoya collaterals but the absence of pial collaterals,

M+P+ to indicate the presence of Moyamoya and pial collaterals). The Table summarizes the demographic data and angiographic scoring for the 11 patients included in the study.

**Cerebrovascular Reactivity by BOLD MR imaging**

MR imaging was performed on a 3T Signa HD clinical MR imaging scanner (GE Medical Systems, Milwaukee, Wisconsin) equipped with 40 mT/m gradient coils and a standard head coil. A standard single-shot BOLD protocol with a spiral readout (TE, 40 ms) was used. The imaging time was 12 minutes for a total acquisition of 320 volumes. Each volume contained 28 sections with a resolution of 3.75 × 3.75 × 4.5 mm. High resolution T1-weighted images were obtained to provide anatomic coregistration. Patients breathed via a tight-fitting mask that was attached to a circuit consisting of a 3 valve manifold and reservoirs for externally supplied gas and exhaled gas. The valves are configured such that external gas is inhaled first and, if the breath size exceeds the gas flow entering the circuit, the balance of inhaled gas is made up with the previously exhaled gas (i.e., rebreathing). External gas is supplied by a custom built computer-controlled gas blender (Respiract; Thornhill Research, Toronto, Canada). It supplies O<sub>2</sub>, and mixtures of CO<sub>2</sub> and N<sub>2</sub> (nitrogen) with O<sub>2</sub>, to achieve target end-tidal CO<sub>2</sub> and end-tidal O<sub>2</sub> independent of breathing pattern.<sup>8</sup> This resulted in near square wave transitions (within 1–3 breaths) and precise, sustained end-tidal gas levels. We used this approach to cycle end-tidal CO<sub>2</sub> between 40 and 50 mmHg in 90 sec cycles while keeping end tidal O<sub>2</sub> at 100 mmHg during BOLD signal acquisition.

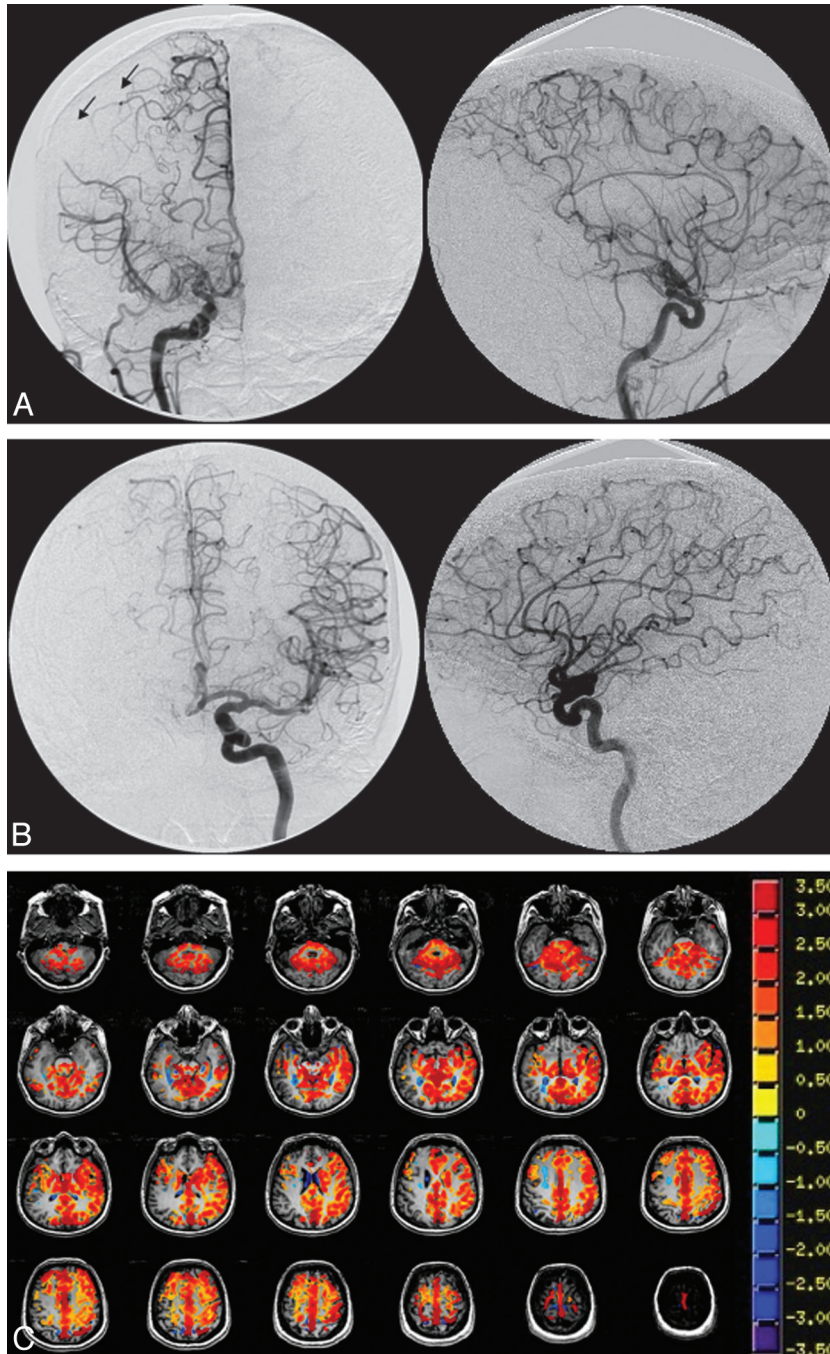
**Data Analysis**

Image analysis was performed by using AFNI, an open-source environment used for processing and displaying functional MR imaging data. BOLD MR imaging data were transformed onto the Talairach coordinate system, and the BOLD data were temporally shifted and correlated with the patient’s CO<sub>2</sub> waveform. A least-squares regression analysis of the BOLD signal intensity versus the CO<sub>2</sub> waveform for each voxel was calculated. For each vascular territory (ACA, MCA, PCA), the CVR for positively and negatively reacting voxels was determined. CVR for each voxel was calculated according to the following:

$$CVR_{\text{voxel}} = \Delta S \div \Delta pCO_2,$$

where ΔS is the change in MR signal intensity for a given voxel that occurs between peak and trough CO<sub>2</sub> levels and ΔpCO<sub>2</sub> is the change in end-tidal CO<sub>2</sub> in mmHg. In healthy brain, CVR is positive, reflect-

BRAIN ORIGINAL RESEARCH



**Fig 1.** A 48-year-old woman who presented with headache. *A*, There is high-grade stenosis of the main trunk of the right MCA with “puff of smoke” vessels in the region of the stenotic trunk. *B*, The left ICA and branches are normal. Angiography indicates a Suzuki grade II right hemisphere and a Suzuki grade 0 left hemisphere. The arrows indicate surface collaterals extending from the right ACA to the right MCA territory. *C*, The CVR map shows absence of reactivity to the CO<sub>2</sub> stimulus (no color) in the right parietal lobe, corresponding to the region of the angiographic collaterals.

ing an increase in CBF in response to increasing pCO<sub>2</sub>. In areas of brain in which blood flow is reduced in response to increasing pCO<sub>2</sub>, CVR is negative. Areas of negative CVR are generally thought to be the result of the vascular “steal” phenomenon, whereby hypercapnea leads to diversion of blood from areas of brain where arterioles are maximally vasodilated and vascular resistance is already minimized to areas of the brain capable of decreasing vascular resistance in response to a CO<sub>2</sub> stimulus.<sup>5</sup>

The mean of all positively reacting voxels in a vascular territory

(Mean CVR<sub>pos</sub>) and the mean of all negatively reacting voxels in a vascular territory (Mean CVR<sub>neg</sub>) were calculated. The Mean CVR<sub>combined</sub> for a given vascular territory was calculated as a weighted average of negative- and positive-reacting voxels as follows:

$$\text{Mean CVR}_{\text{combined}} = f_{\text{neg}} \times \text{Mean CVR}_{\text{neg}} + f_{\text{pos}} \times \text{Mean CVR}_{\text{pos}},$$

where  $f_{\text{neg}}$  and  $f_{\text{pos}}$  are the fraction of negatively and positively reacting voxels respectively.



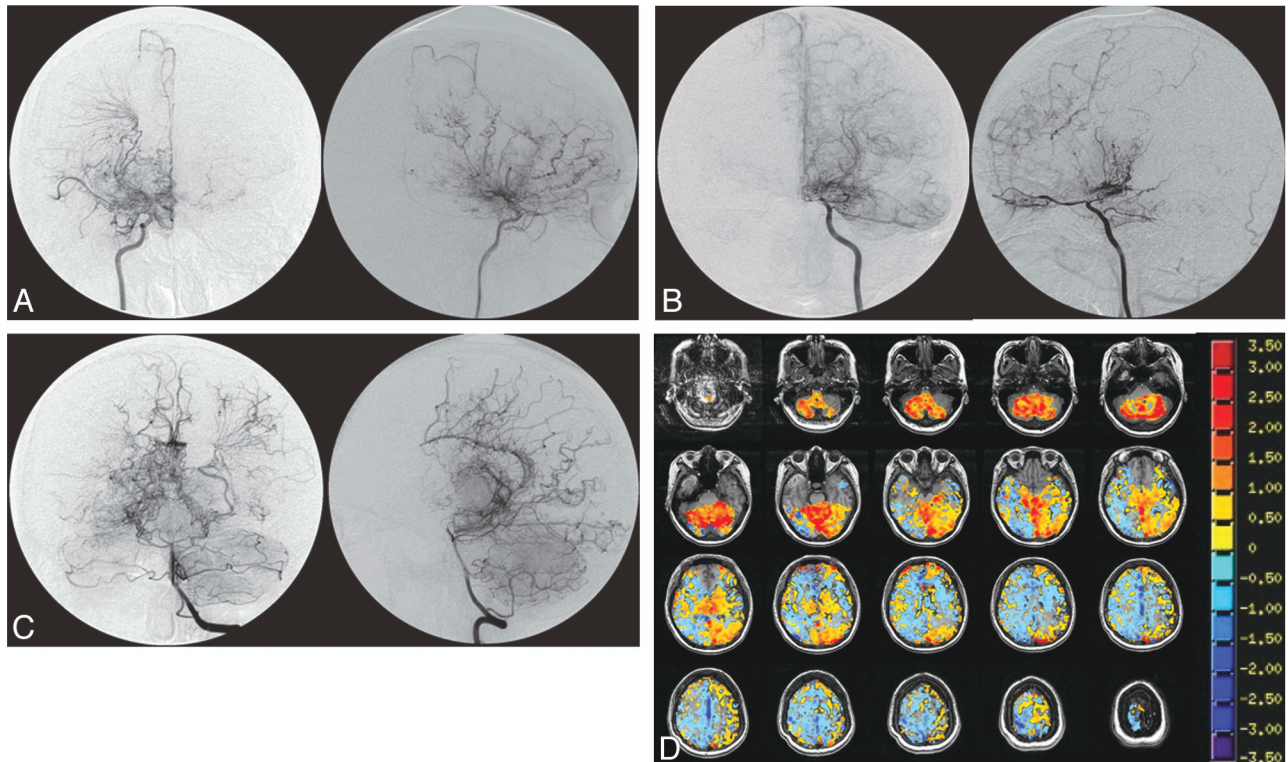


**Fig 2.** A 35-year-old woman who presented with TIA consisting of left hemiparesis. *A–C*, The angiograms indicate severe stenosis/occlusion of the distal ICAs bilaterally, with extensive Moyamoya vessels consistent with Suzuki grade IV bilaterally. The left vertebral injection (*C*) shows extensive pial collateralization from the posterior circulation to the ACA and MCA territories. However, the right hemisphere is not as well supplied as the left. *D*, This finding is supported by the CVR map, which shows a greater extent of steal phenomena (blue pixels) in the right hemisphere compared with the left. Notice the preservation of reactivity in the relatively well-supplied cerebellum.

### Statistical Analysis

Statistical analysis was performed by using Prism (GraphPad Software, La Jolla, California). The correlation between Mean  $CVR_{combined}$  for the MCA and ACA territories and the modified Suzuki score, and the correlation between Mean  $CVR_{combined}$  for combined ACA and MCA territories and presence of Moyamoya and pial collaterals were calculated with a Pearson correlation coefficient. One-way ANOVA was performed to compare the Mean  $CVR_{combined}$  for vascular territories with different Suzuki scores. An unpaired *t* test was used to compare the Mean  $CVR_{combined}$  for vascular territories with and without Moyamoya or pial collaterals.

### Results

The study group comprised 7 females and 4 males with an age range between 10 and 48 years. Five patients had unilateral disease and 6 patients had bilateral disease. A total of 66 vascular territories were analyzed (11 each of the right and left ACA, right and left MCA, and right and left PCA). CVR maps are shown for 2 patients with varying degrees of Moyamoya disease and the corresponding conventional angiograms for the affected vascular territories (Figs 1 and 2). The CVR maps qualitatively show a correlation between regional changes in CVR and angiographic features of Moyamoya disease.

The Mean  $CVR_{combined}$  for MCA and ACA territories was plotted against the degree of Moyamoya disease as observed on conventional angiography and measured by the modified Suzuki score (Fig 3). There was good correlation between

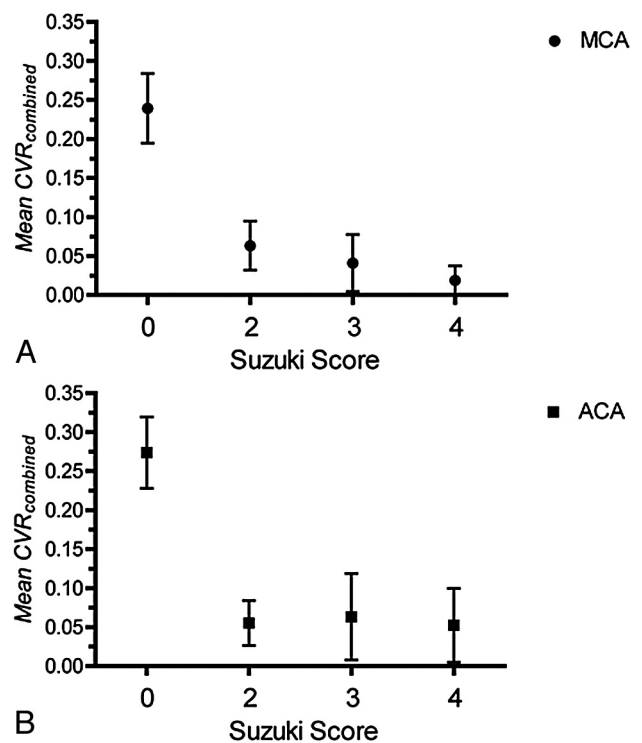


**Fig 3.** Relationship between Mean  $CVR_{combined}$  versus disease severity as measured by the modified Suzuki score. *A*, Mean  $CVR_{combined}$  versus the Suzuki score for the MCA territory. *B*, Mean  $CVR_{combined}$  versus the Suzuki score for the ACA territory.

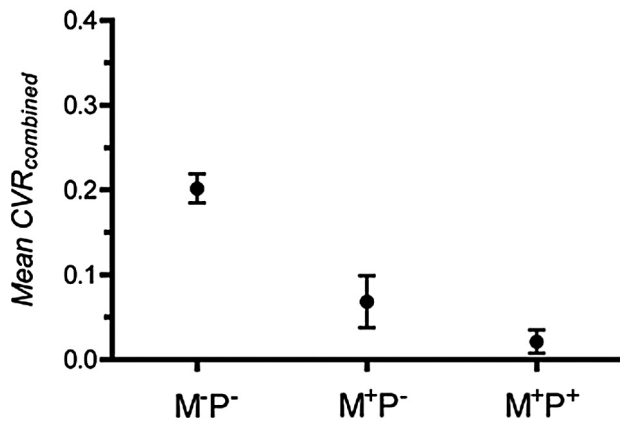


**Fig 4.** Correlation between Mean CVR<sub>combined</sub> for MCA and ACA territories and the presence of pial or Moyamoya collaterals. M-P- indicates the absence of Moyamoya or pial collaterals, M+P- indicates the presence of Moyamoya collaterals but the absence of pial collaterals, and M+P+ indicates the presence of Moyamoya and pial collaterals.

Mean CVR<sub>combined</sub> and Suzuki class for MCA and ACA territories (Pearson correlation coefficient,  $-0.7560$  and  $-0.6140$ , respectively); however, the correlation was better for the MCA territory. Vascular territories with Suzuki score  $>0$  had a statistically significant lower CVR score compared with disease-free areas (1-way ANOVA,  $P < .0001$  for MCA and ACA territories). There was a decreasing trend of Mean CVR<sub>combined</sub> with increasing disease score, but the difference was not statistically significant.

The Mean CVR<sub>combined</sub> was calculated for combined ACA and MCA territories with Moyamoya and pial collaterals (M+P+), Moyamoya collaterals alone (M+P-), and no collaterals (M-P-) (Fig 4). There was a good correlation between Mean CVR<sub>combined</sub> and the presence of collateral vessels (Pearson correlation coefficient,  $-0.7466$ ). Territories with vessel collaterals had significantly lower Mean CVR<sub>combined</sub> (Mean CVR<sub>combined</sub>  $\pm$  SE =  $0.068 \pm 0.031$  and  $0.021 \pm 0.013$  for M+P- and M+P+, respectively) compared with territories with no collaterals (Mean CVR<sub>combined</sub>  $\pm$  SE =  $0.20 \pm 0.017$ ). Territories containing Moyamoya and pial collaterals (M+P+) had a lower Mean CVR<sub>combined</sub> compared with territories with Moyamoya vessels alone (M+P-), but this difference was not statistically significant ( $P = .11$ , unpaired  $t$  test).

To examine the dependence of CVR on the extent of vascular steal, we generated plots of Mean CVR<sub>pos</sub>, Mean CVR<sub>neg</sub>, and Mean CVR<sub>combined</sub> versus the fraction of negatively reacting voxels ( $f_{neg}$ ) for all ACA, MCA, and PCA territories. Vascular territories affected by Moyamoya disease (Suzuki  $>0$ ) have more vascular steal (higher  $f_{neg}$ ) compared with disease-free territories (Suzuki = 0). A nonlinear decrease in Mean CVR<sub>pos</sub> with  $f_{neg}$  was found (Fig 5A). An exponential decay with a plateau of 0 was fitted to the data ( $R^2 = 0.45$ ). A similar trend for Mean CVR<sub>combined</sub> against  $f_{neg}$  (Fig 5B) was fitted to an exponential decay with a plateau of  $-0.09$  ( $R^2 = 0.72$ ). Extrapolating from this fit, the x-intercept (Mean CVR<sub>combined</sub> = 0) occurs with  $f_{neg} = 0.52$ . A plot for Mean CVR<sub>neg</sub> illustrates the independence of Mean CVR<sub>neg</sub> over a wide range of  $f_{neg}$  values (Fig 5C).

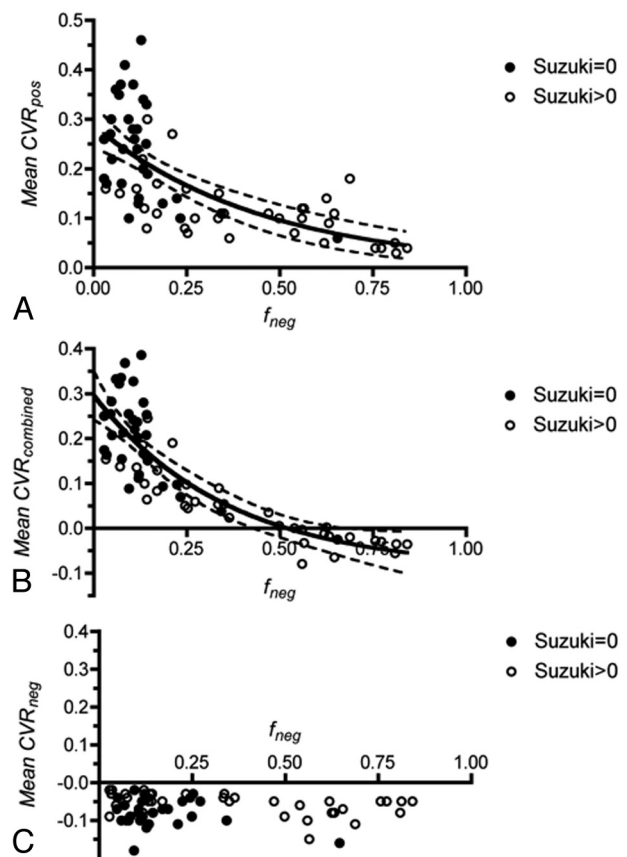


**Fig 5.** Relationship between Mean CVR<sub>pos</sub>, Mean CVR<sub>combined</sub>, Mean CVR<sub>neg</sub>, and the degree of vascular steal ( $f_{neg}$ ) for all ACA, MCA, and PCA territories. Closed circles represent vascular territories with a Suzuki score of 0, and open circles, Suzuki  $>0$ . A, Mean CVR<sub>pos</sub> versus  $f_{neg}$ . B, Mean CVR<sub>combined</sub> versus  $f_{neg}$ . An exponential decay has been fitted to the data. The dotted lines indicate the 95% confidence band. C, Mean CVR<sub>neg</sub> versus  $f_{neg}$ .

## Discussion

Measurement of CVR with BOLD MR imaging and the CO<sub>2</sub> rebreathing circuit used in the current study has a number of advantages over existing methods. Nuclear medicine techniques such as PET and SPECT have poor spatial and temporal resolution and involve the administration of radioactive tracers. Changes in CBF measured with CT perfusion have been shown to correlate well with angiographic scoring of Moyamoya disease.<sup>4</sup> The accurate quantification of CBF by using CT perfusion is dependent on an AIF, which is difficult to define in circulation affected by Moyamoya disease. In addition, studies that rely on breath-hold or acetazolamide stress cannot reproducibly create changes in end-tidal pCO<sub>2</sub> and, therefore, cannot accurately quantify CVR. BOLD MR imaging is a readily accessible technique that can produce quantitative maps of CVR with high temporal and spatial resolution, requires no radioactive tracer, and is not dependent on an AIF. Furthermore, the rebreathing technique used in the current study produces reproducible changes in end-tidal pCO<sub>2</sub>, allowing truly quantitative and accurate mapping of CVR.

Using the BOLD MR imaging technique with the rebreathing circuit, we found a good correlation between Mean CVR<sub>combined</sub> and the Suzuki score. The Mean CVR<sub>combined</sub> decreases with increasing Suzuki score; however, the difference was not statistically significant between vascular territories for

a Suzuki score of  $>0$ . This is not completely unexpected because angiographic scoring of upstream feeding vessels may not adequately reflect the perfusion in downstream tissue. Furthermore, we have shown that the effect on Mean  $CVR_{combined}$  is diminished as disease burden increases (Fig 5B), so while a significant difference between Mean  $CVR_{combined}$  for a vascular territory with a Suzuki score of 0 and a Suzuki score of  $>0$  may be significant, we expect a smaller difference between vascular territories with non-zero Suzuki scores.

The correlation between CVR and the presence of Moyamoya and pial collaterals suggests that the presence of these vessels is associated with poor vascular reactivity that is not adequately compensated by collateralization. Vascular territories with pial and Moyamoya vessels had a nonsignificant but lower Mean  $CVR_{combined}$  compared with vascular territories with Moyamoya vessels alone. The presence of pial collaterals may, therefore, represent a more severe disease burden as measured by Mean  $CVR_{combined}$ ; however, further measurements will be needed to clarify this relationship.

Measurements indicate that a nonlinear relationship exists between Mean  $CVR_{pos}$  and  $f_{neg}$  (Fig 5A). For small values of  $f_{neg}$ , there is an initial large decrease in Mean  $CVR_{pos}$  for small changes in  $f_{neg}$ . As  $f_{neg}$  increases, the effect on Mean  $CVR_{pos}$  is diminished. In contrast, the mean reactivity of negatively reacting voxels (Mean  $CVR_{neg}$ ) is relatively constant over a range of  $f_{neg}$ . The Mean  $CVR_{combined}$  is, therefore, predominantly affected by changes in Mean  $CVR_{pos}$  for small values of  $f_{neg}$ . As the amount of steal increases in a given vascular territory, the decrease in Mean  $CVR_{combined}$  is mainly determined by the increasing extent of steal ( $f_{neg}$ ) and not significantly by decreasing Mean  $CVR_{pos}$  or Mean  $CVR_{neg}$ . No attempt has been made to mathematically model the relationship between CVR and  $f_{neg}$ , but the results presented here demonstrate a reproducible relationship between these parameters in all vascular territories studied and in multiple patients.

There was a decreasing trend between Mean  $CVR_{combined}$  and increasing Suzuki score and vessel collateralization, but the difference was not statistically significant. Statistically sig-

nificant differences may exist; however, the study was limited because of the small number of patients analyzed. Other limitations of this study were the deficiency of patients with mild Moyamoya disease (Suzuki = 1) and the retrospective nature of the study.

## Conclusions

BOLD MR imaging in combination with precision control of end-tidal  $pCO_2$  and  $pO_2$  is an easily implemented technique that can produce reproducible and quantitative maps of CVR. In the present work, we have demonstrated how this technique correlates well with existing measures of Moyamoya disease burden by using conventional angiography and, therefore, validates the use of BOLD MR imaging for this purpose. However BOLD MR imaging takes this correlation one step further by providing truly quantitative maps of the spatial severity of Moyamoya disease.

## References

1. So Y, Lee HY, Kim SK, et al. **Prediction of the clinical outcome of pediatric Moyamoya disease with postoperative basal/acetazolamide stress brain perfusion SPECT after revascularization surgery.** *Stroke* 2005;36:1485–89. Epub 2005 Jun 9
2. Kuwabara Y, Ichiya Y, Sasaki M, et al. **Response to hypercapnia in Moyamoya disease: cerebrovascular response to hypercapnia in pediatric and adult patients with Moyamoya disease.** *Stroke* 1997;28:701–07
3. Yamamoto S, Watanabe M, Uematsu T, et al. **Correlation of angiographic circulation time and cerebrovascular reserve by acetazolamide-challenged single photon emission CT.** *AJNR Am J Neuroradiol* 2004;25:242–47
4. Kang KH, Kim HS, Kim SY. **Quantitative cerebrovascular reserve measured by acetazolamide-challenged dynamic CT perfusion in ischemic adult Moyamoya disease: initial experience with angiographic correlation.** *AJNR Am J Neuroradiol* 2008;29:1487–93. Epub 2008 May 22
5. Mandell DM, Han JS, Poubanc J, et al. **Mapping cerebrovascular reactivity using blood oxygen level-dependent MRI in patients with arterial stenocclusive disease: comparison with arterial spin labeling MRI.** *Stroke* 2008;39:2021–28
6. Vesely A, Sasano H, Volgyesi G, et al. **MRI mapping of cerebrovascular reactivity using square wave changes in end-tidal  $PCO_2$ .** *Magn Reson Med* 2001;45:1011–13
7. Mugikura S, Takahashi S, Higano S, et al. **Predominant involvement of ipsilateral anterior and posterior circulations in Moyamoya disease.** *Stroke* 2002;33:1497–500
8. Slessarev M, Han J, Mardimae A, et al. **Prospective targeting and control of end-tidal  $CO_2$  and  $O_2$  concentrations.** *J Physiol* 2007;581(Pt3):1207–19